

Pb(Zr_{0.95}Ti_{0.05})O₃ powders prepared by aqueous Pechini method using one-step pyrolysis process: characterization and porous ceramics

Shaojun Qiu · Chao Gao · Xiaodong Zheng · Jin Chen ·
Chen Yang · Xiaoxian Gan · Huiqing Fan

Received: 15 May 2007 / Accepted: 29 January 2008 / Published online: 8 March 2008
© Springer Science+Business Media, LLC 2008

Abstract Zr-riched lead zirconate titanate, Pb(Zr_{0.95}Ti_{0.05})O₃ (PZT 95/5) powders were prepared using lead acetate, zirconium oxynitrate, and titanium sulfate by aqueous Pechini method. The chelation behaviors of metallic ions and citric acid were investigated and the development of the phase formation of perovskite structure was detected. PZT 95/5 powders were obtained directly from the as-synthesized gels by one-step pyrolysis process at 450 °C for 10 h. Perovskite phase was formed at about 450 °C and no distinct intermediates were obtained. There were some carbonates as impurities but they did not affect the formation of the complete perovskite phase of PZT 95/5 ceramics after sintering at 1,100–1,150 °C for 2 h. The decomposition of few organic residues among the one-step pyrolyzed powders could form uniform porous structure and the formation mechanism of porous ceramics was also presented.

Introduction

Solid solutions of lead zirconate (PZ) and lead titanate (PT) in different proportions have found many important applications due to their piezoelectric and ferroelectric properties. For a particular composition having a Zr:Ti

molar ratio of 95:5, Pb(Zr_{0.95}Ti_{0.05})O₃ (PZT 95/5), it was proposed as a source of pulsed power for neutron generator through shock-wave compression [1, 2].

Soft chemical methods, including Pechini method, have shown its versatility in several alternative systems for preparing well-characterized mixed-oxide powders [3–8]. PZT powders have been successfully prepared by many researchers [9, 10]. Tas [11] and Gajbhiye et al. [12] prepared nano-sized PZT powders from water-soluble chlorides by the homogeneous precipitation via urea decomposition. Abreu et al. [13] controlled pH value at 6.5 by the decomposition of urea to get PZT 52/48 powders presenting spherical uniform-sized particles of about 100 nm. However, there have few studies on the synthesis of PZT 95/5 powders using Pechini method. In previous research, we have presented the effects of the molecular weight of polyesters formed by polymerization of citric acid and ethylene glycol on the evolution of phase formation and agglomerate of PZT 95/5 powders prepared by Pechini method [14]. In the present study, PZT 95/5 powders were prepared by aqueous Pechini method and a one-step pyrolysis process at lower temperature was introduced instead of the normal two-step pyrolysis process. Porous PZT 95/5 ceramics could be prepared by the powders derived from one-step pyrolysis process without additional pore formers. Furthermore, the formation mechanism of porous ceramic by elimination of produced gases was presented.

Experimental

Materials and process

Lead acetate (Pb(CH₃COO)₂ · 3H₂O, ≥99.0%), zirconium oxynitrate (ZrO(NO₃)₂ · 2H₂O, ≥99.0%), and titanium

S. Qiu (✉) · C. Gao · X. Zheng · X. Gan
Xi'an Modern Chemistry Research Institute, Xi'an 710065,
China
e-mail: shaojqiu@yahoo.com

J. Chen · C. Yang · H. Fan
State Key Laboratory of Solidification Processing, School
of Materials Science and Engineering, Northwestern
Polytechnical University, Xi'an 710072, China

sulfate ($\text{Ti}(\text{SO}_4)_2$, $\geq 96.0\%$) were used as metallic cations sources. Citric acid monohydrated (CA, AR) and ethylene glycol (EG, AR) were used as chelating agents. All materials are purchased from Sinopharm Chemical Reagent Co., Ltd., Shanghai, China. In order to eliminate the influence of chlorine on the crystalline behavior of PZT 95/5 powders, in the present study, zirconium oxynitrate substitute for zirconium oxychloride as zirconium sources. Figure 1 shows the flowchart for the process of PZT 95/5 ceramics by Pechini method prepared powders. The molar ratio of the $[\text{CA}]:[\text{EG}]:[\text{Pb}]:[\text{Zr}]:[\text{Ti}]$ is 160:160:20.6:19:1. The lead amount is 3% excess in molar ratio to prevent lead volatilization in sintering process.

CA solution was prepared by mixing citric acid (105 g, 0.50 mol) in 100 mL of deionized water at 70 °C. Titanium sulfate (0.78 g, 3.12×10^{-3} mol) was then added to this solution, which was stirred until complete dissolution. Aqueous zirconium oxynitrate solution was prepared by

mixing zirconium oxynitrate (15.87 g, 5.94×10^{-2} mol) in 50 mL of deionized water and was then added to the previous solution. There was no precipitation and additionally, the solution was stirred at 70 °C for 1 h. Aqueous lead acetate solution was prepared by mixing lead acetate (24.47 g, 6.44×10^{-2} mol) in 50 mL of deionized water at 70 °C and was then added to the titanium and zirconium citrate solution. The metallic chelates solution was stirred for 2 h and then EG (31 g, 0.50 mol) was added. The temperature was gradually raised to 150 °C for polyesterification reaction and retained at this temperature for 2 h.

The hybrid inorganic–organic polymerized gels were then followed the one-step pyrolysis process. It was heated at a $5 \text{ }^\circ\text{C min}^{-1}$ heating rate, in static air, to 450 °C and kept at this temperature for 10 h to prepare PZT 95/5 powders (referred as Powder A). Powder A was calcined at higher temperatures to obtain Powder B1 (at 700 °C for 10 h), Powder B2 (at 800 °C for 2 h), and Powder B3 (at 800 °C for 3.7 h). Powders were cold isostatically pressed at 100 MPa into disks and was sintered at 1,050, 1,100, and 1,150 °C for 2 h in a sealed alumina crucible with lead zirconate atmosphere powder.

Characterization

Thermogravimetric analysis (TGA) in air was performed on a TA TGA 2950 from 25 to 800 °C at a heating rate of $10 \text{ }^\circ\text{C min}^{-1}$, with an air flow rate of 200 mL min^{-1} . Fourier transform infrared spectrum (FTIR) in the range of $400\text{--}4,000 \text{ cm}^{-1}$ was recorded using KBr pellets on a Nicolet-60SXR-FTIR spectrometer with spectrum resolution of 4 cm^{-1} . The powders and ceramics were characterized by X-ray diffractometry (XRD, X'Pert PRO MPD) using Co radiation ($\lambda = 1.78897 \text{ \AA}$) at 35 kV and 40 mA, from 20° to 80° of 2θ , to identify the various phases formed. The average crystallite dimension was estimated from the most intense diffraction peak by means of the Scherrer equation. Field emission scanning electron microscopy (FESEM, JEOL JSM 6700F) and scanning electron microscopy (SEM, JEOL JSM-5610LV) were used to obtain the microstructures of the powders and ceramics on fresh fracture faces, respectively. The metals contents were determined by Energy Dispersive Spectrometry (EDS). The densities of fired pieces were determined by the water displacement method.

Results and discussion

One-step pyrolysis process

For Pechini method, the normal pyrolysis process includes a two-step thermal decomposition to obtain powders. First,

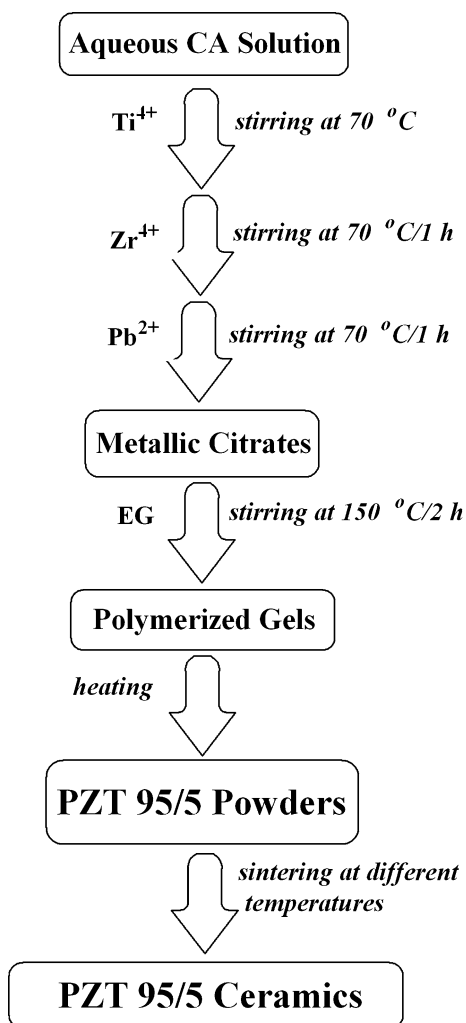


Fig. 1 Flowchart for the preparation of PZT 95/5 powders and porous ceramics

most of organic matters pyrolyzes at a lower temperature, such as 300–500 °C, to obtain a polymeric precursor. Then, the polymeric precursor calcines at a higher temperature, such as 500–900 °C, to form a certain phase structure. The few organic residues could decompose completely in the second step. In this study, we introduce a one-step pyrolysis process at lower temperature to obtain powders directly form the polymeric gels by Pechini method, i.e., in static air, the polymeric gels were calcined at 450 °C for 10 h. The one-step pyrolysis process could prevent the introduction of impurities and simultaneously making the overall process become power and time economic.

XRD results of PZT 95/5 powders

The XRD patterns of the powders calcined at different conditions are shown in Fig. 2. The perovskite PZT 95/5 is predominant in the sample with some carbonates remained after calcination at 450 °C for 10 h by one-step pyrolysis process (Powder A, Fig. 2a), indicating incomplete decomposition of the gels induced by the low temperature. In order to eliminate the secondary phases, higher calcination temperatures are applied for Powder A. The results (Fig. 2b–d) show that the higher calcination temperature neither improves the crystallinity of PZT 95/5 powders, nor reduces the amount of carbonates. Blanco López et al. [15] have indicated that the complete elimination of BaCO₃ at 1,000 °C was not sufficient.

Thermal decomposition of the polymeric gels upon rapid heat-treatment yields an impurity of oxocarbonate and the crystal structure of the oxocarbonate is unknown [16]. These incompleteness does not affect the formation of the complete perovskite PZT 95/5 ceramics as seen later.

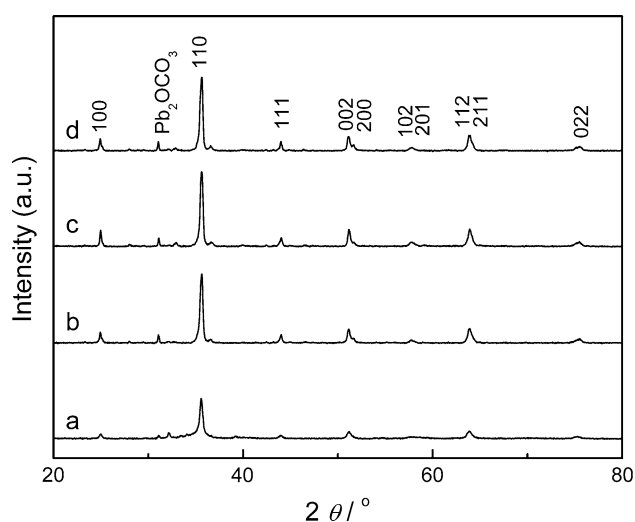


Fig. 2 XRD patterns of PZT 95/5 powders ($\lambda = 1.78897 \text{ \AA}$) calcined at different conditions. (a) Powder A; (b) Powder B1; (c) Powder B2; and (d) Powder B3, respectively

Table 1 The mean crystallite size of PZT 95/5 powders

Calcination conditions	Powder A 450 °C/ 10 h	Powder B1 450 °C/10 h and then 700 °C/10 h	Powder B2 450 °C/10 h and then 800 °C/2 h	Powder B3 450 °C/10 h and then 800 °C/3.7 h
Mean size (nm)	33	29	29	27

By applying the Scherrer formula to the peak at 35.6° of 2θ , the mean crystallite sizes of PZT 95/5 powders are shown in Table 1. When Powder A is calcined at higher temperature, the mean crystallite size is reduced as the temperature and time increased. It could be resulted from the decomposition of the organic residues among Powder A (see later). Comparing with our previous results [14], more intense and sharper diffraction peaks appear in this study even for the powders calcined at 450 °C.

There are no TiO₂ and/or ZrO₂ detected in Fig. 2. From the XRD results, we could conclude that the chelated structure of CA and metallic ions in the gels undergoes a one-step decomposition process to form the perovskite PZT 95/5.

FTIR of gels and PZT 95/5 powders

Figure 3 shows the FTIR spectra of the gels and powders calcined at different temperatures. Three bands related to carboxylate stretching modes are observed at 1,732, 1,635, and 1,398 cm⁻¹ of the gels (Fig. 3a) [13, 17]. The band at 1,732 cm⁻¹ could be assigned to the C=O stretching mode of the ester which was formed by polyesterification reaction of CA and EG. The 1,635 cm⁻¹ band could be assigned to the asymmetric COO⁻ stretching mode for a

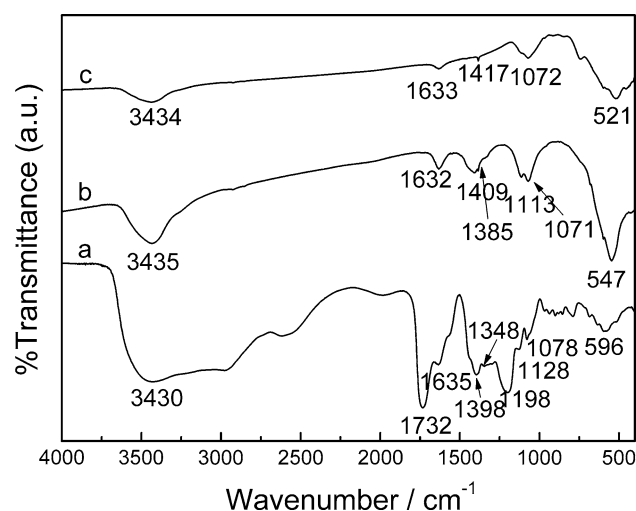


Fig. 3 FTIR spectra of gels and PZT 95/5 powders. (a) Polymeric gels; (b) Powder A; and (c) Powder B2, respectively

unidentate complex, formed from the chelation of carboxyl group of CA and metallic ions. The $1,398\text{ cm}^{-1}$ band could be assigned to the symmetric COO^- stretching mode from the chelation of carboxyl group of CA and metallic ions. The bands of $1,635$ and $1,398\text{ cm}^{-1}$, with $\Delta\nu = 237\text{ cm}^{-1}$, suggest that the gels contain one unidentate group in the structure [18, 19]. The other bands at $1,500$ – 850 and $3,500$ – $2,600\text{ cm}^{-1}$ are attributed to the adsorbed water, polymeric network and OH, CH_2 , and CH groups, respectively. The bands below 650 cm^{-1} are assigned to metal oxygen-stretching mode from the chelation of CA and metallic ions.

FTIR spectrum of Powder A is illustrated in Fig. 3b. When the gel is heated at $450\text{ }^\circ\text{C}$ for 10 h, the band at $1,632\text{ cm}^{-1}$ is attributed to the COO^- stretching in unidentate metallic complex formed between carboxyl group and metallic ions [17]. This unidentate metallic complex is still present in the powders even after calcination at $450\text{ }^\circ\text{C}$ for 10 h, suggesting that the strong chelating ability provided by the α -hydroxylic acid groups of CA can stabilize different metal ions simultaneously within one molecule or complex [20]. The band at $1,409\text{ cm}^{-1}$ is symmetric stretching vibrations for carboxylate ions (COO^-). Comparing with Fig. 3a, the C=O group stretching ($1,732\text{ cm}^{-1}$) is disappeared, suggesting that the polyesters formed by CA and EG have begun to decompose into derivative compounds. The bands at $1,113$ and $1,071\text{ cm}^{-1}$ are assigned to the carbonate ions (CO_3^{2-}). The band at $3,435\text{ cm}^{-1}$ is attributed to the water adsorbed on the surface of powders. It will be confirmed by thermal analysis (see later).

When Powder A is calcined again at higher temperature, the aspects of infrared spectra have no obvious changes after and before calcined at higher temperatures but the related absorption intensity decreasing (Powder B2, Fig. 3c). The unidentate metallic complex formed between carboxyl group and metal ions and the carbonate ions are still remained among the powders. The FTIR results accord with the XRD results well. Blanco López et al. [15] and our XRD and FTIR results confirm the presence of carbonates even after calcined the one-step pyrolyzed powders at $800\text{ }^\circ\text{C}$ for 2 h.

Thermal analysis of PZT 95/5 powders by one-step pyrolysis process

The differential scanning calorimetry (DSC) curve of the gels obtained by Pechini method has been presented previously [14]. The elimination of the excess CA and EG among the macromolecules network and the thermal decomposition of the polyester chains could be clearly distinguished. For Powders A, the TGA curve (Fig. 4) shows a continuous mass decrease between 25 and $280\text{ }^\circ\text{C}$ and no obvious mass loss above $280\text{ }^\circ\text{C}$. There is a

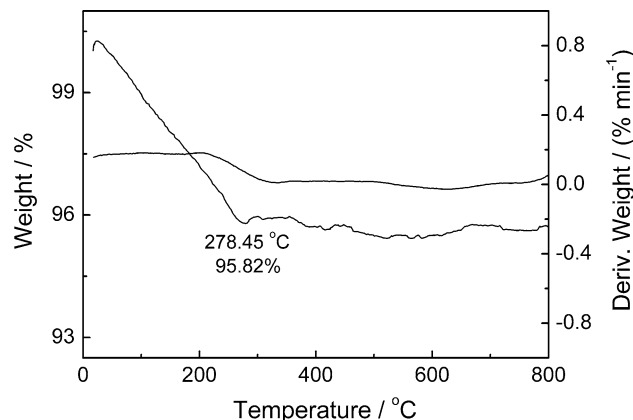


Fig. 4 TGA curve of Powder A

reduction in weight about 4.18%, which indicates that most of organic species decomposes by the one-step pyrolysis process in this study.

The data collected from Fig. 4 are used to analyze the thermal process of PZT 95/5 powders by one-step pyrolysis process. From the previous DSC results, the weight loss before $150\text{ }^\circ\text{C}$ is associated to the elimination of free water. Therefore, there is about 2% of free water (mass ratio) among the powders and about 2% organic matters (mass ratio) among Powder A. Upon thermal treatment, free water escaped from the surface of the powders and then the organic residues oxidize to carbon dioxide and water.

The overall amount of inorganic part is 21.52 g (in $\text{Pb}(\text{Zr}_{0.95}\text{Ti}_{0.05})\text{O}_3$ formula) and the organic residues are about 2% (in mass ratio from the data of Fig. 4) after one-step pyrolysis process at $450\text{ }^\circ\text{C}$ for 10 h, so the organic residues among PZT powders are about 0.43 g. The theoretical amount of organic part is 100 g (subtract the theoretical water formed from the overall organic matters added, $105 + 31 - 18 \times (0.5 \times 3 + 0.5) = 100$). Therefore, there are about 99.6% ($(100 - 0.43)/100$) of organic matters decompose in the one-step pyrolysis process.

Microstructure of PZT 95/5 powders

Lessing [6] has concluded that it would be impossible to obtain unagglomerated powders through calcination of a dense and rigid polymer material; we also observed that the powders are agglomerates previously. Leite et al. [21] concluded that the particle size obtained by Pechini method is related to the polymer thermal decomposition. We have presented the effect of the molecular weight of polyester formed by CA and EG on the agglomerates and particle size of the PZT 95/5 powders previously [14]. The molecular weight of polyester plays a key role in the crystalline size, morphology and phase formation. In

Fig. 5, we could see that the particle size is smaller for the powders calcined at higher temperature. After calcination at 450 °C for 10 h by one-step pyrolysis process, Powder A is agglomeration and the particles are about 1 μm . When Powder A was calcined at 800 °C for 2 h again, the obtained Powder B2 is still agglomeration but the particle size decreases to about 100–200 nm. It could be attributed to the decomposition of the remained organic matters among the powders.

According to EDS analyses, Pb:Zr:Ti of Powder A and Powder B2 were close to 20.7:19.2:1 and 20.3:19.1:1 (all in molar ratio), respectively.

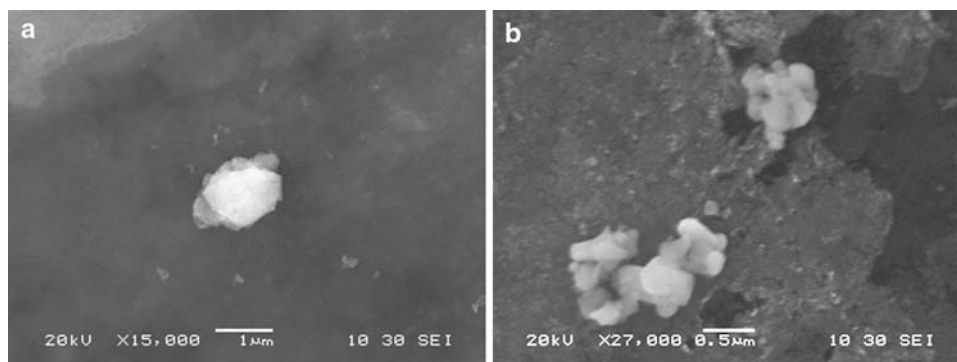
XRD of PZT 95/5 ceramics

Figure 6 shows the XRD results of ceramics sintered at different temperatures. For Powder A, XRD patterns show complete perovskite structure of the ceramics sintered at 1,100–1,150 °C for 2 h (Fig. 6b, c). It is notable to see the impurities in the powders have been eliminated completely. In order to examine the effect of heat-treatment process of the powders on the phase structure of the ceramics, Powder B2 was sintered at 1,050 °C for 2 h. The result shows complete perovskite phase and sharper peak of ceramics sintered for Powder B2 (Fig. 6d). The full waves at half maximum (FWHM) of the strongest peaks of the ceramics sintered at different temperatures are listed in Table 2. For Powder A, a decrease in the FWHM with the sintering temperature is due to the crystalline growth at higher temperatures. When the one-step pyrolyzed powders are recalcined at higher temperature (Powder B2), narrower FWHM is presented, which means larger particle size. So we could prepare ceramics having more little crystalline particle size at same sintering temperature for the one-step pyrolyzed powders by adjusting the pyrolysis temperature.

Porous PZT 95/5 ceramics without pore formers

In previous communication, we have presented the formation of porous ceramics without additional pore formers from chemically prepared powders [22]. In the same way,

Fig. 5 FESEM micrographs of PZT 95/5 powders. (a) Powder A and (b) Powder B2



porous PZT 95/5 ceramics were obtained in this study. The densities of ceramics sintered at different temperatures are shown in Table 2. The highest density is got after sintered at 1,150 °C for 2 h for Powder A. For the Powder B2, its density is higher than Powder A at the same sintering condition. It could be attributed to the organic residues among Powder A (see Fig. 4). The decomposition of the organic residues produces large amount of water vapor and carbon dioxide, and these gases escape from the green bodies forming pores in the ceramics. Therefore, at low

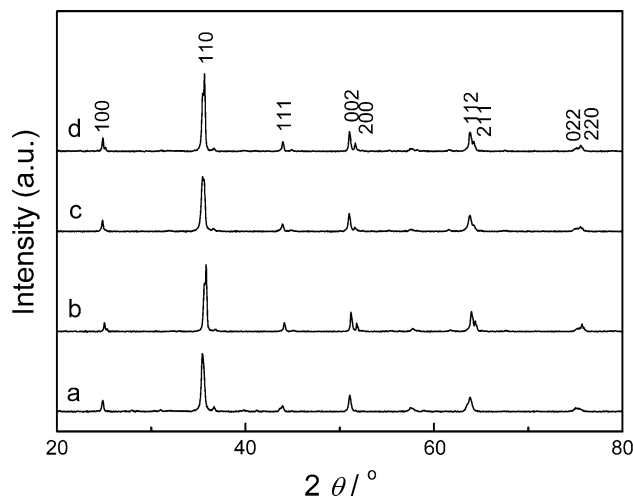


Fig. 6 XRD patterns of PZT 95/5 ceramics ($\lambda = 1.78897 \text{ \AA}$) sintered at different temperatures for 2 h. (a) 1,050 °C, (b) 1,100 °C and (c) 1,150 °C for Powder A, and (d) 1,050 °C for Powder B2, respectively

Table 2 FWHM and density of the ceramics sintered at different conditions

Sintering conditions	Powder A			Powder B2
	1050 °C/ 2 h	1100 °C/ 2 h	1150 °C/ 2 h	1050 °C/ 2 h
FWHM ($^{\circ}$ of 2θ)	0.2273	0.1948	0.1299	0.1299
Relative density (%)	77	88	92	89

temperature (1,050 °C) the ceramics have porous structures and low densities. When increasing the sintered temperatures, the formed pores shrink and the densities increase.

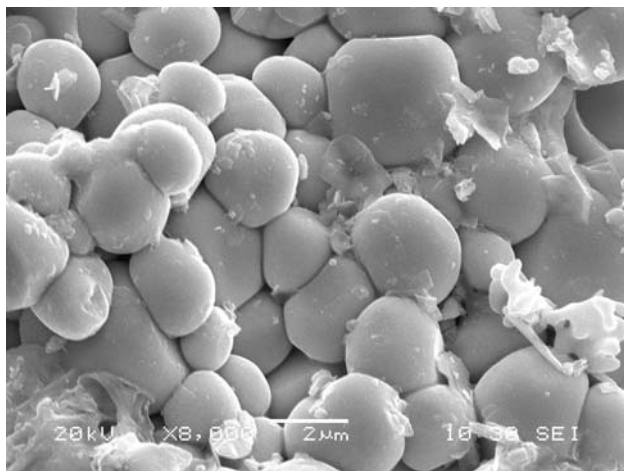
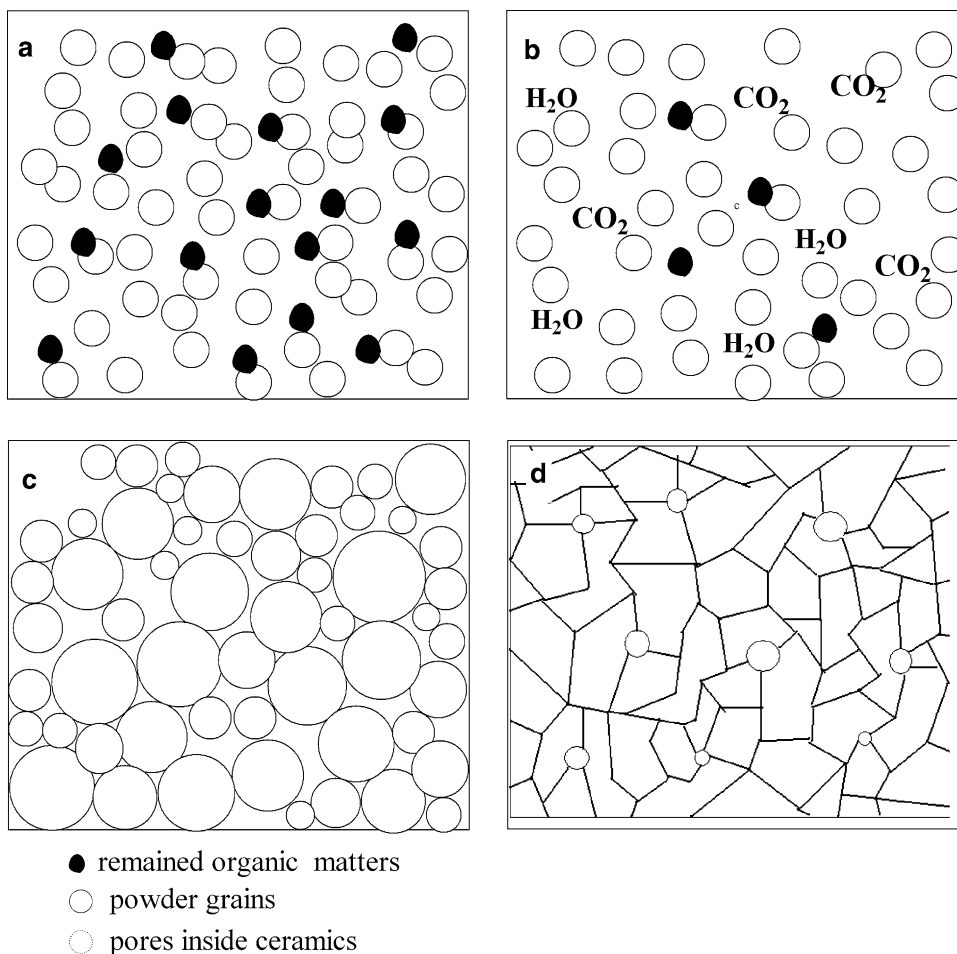


Fig. 7 SEM micrograph of PZT 95/5 ceramics sintered at 1,100 °C for 2 h of Powder A

The microstructures of the ceramics determined by SEM on a fresh fracture surface are presented in Fig. 7. For Powder A, when the ceramics are sintered 1,100 °C for 2 h, the dark areas in SEM micrographs are pores and homogeneous dispersion. It should be noted that the microstructure also had minute pores about 0.5–2 µm in size. The sintered materials have fine-grain structures with individual grain of 1–3 µm in size.

The formation mechanism of porous ceramics without additional pore formers is shown in Fig. 8. In the initial sintering, the organic residues among the powders decompose to large amount of water vapor and carbon dioxide, and these gases escape from the green bodies forming pores in the ceramics [22]. In this stage the compacts behave volume expansion and low density. Then the grain growth and densification plays a key role and the compacts begin shrink. Pores could be eliminated partially and the density of compacts increases. In the final stage of sintering, a balance of grain growth, densification and pore elimination could result in the porous ceramics. Unlike the burn out of additional pore formers, such as microcrystalline cellulose (MCC) rods and polymethyl methacrylate (PMMA) spheres [23, 24], the decomposition of organic

Fig. 8 Schematic illustration of formation of porous PZT 95/5 ceramics. (a) Cold isostatically pressed compacts and the remained organic matters dispersed uniformly among the powders; (b) the organic matters decompose to large amount of water vapor and carbon dioxide and resulting volume expansion and low density; (c) grain growth, densification and pore elimination; and (d) balance of grain growth, densification and pore elimination resulting the porous ceramics



residues among PZT powders could obtain homogeneous pores.

Conclusion

Using zirconium oxynitrate instead of zirconium oxychloride as zirconium sources by aqueous Pechini method, PZT 95/5 powders are obtained at lower temperature (about 450 °C) by one-step pyrolysis process and there are few secondary phases accompanied with perovskite PZT 95/5. Though more than 99% of organic matters decompose in one-step pyrolysis process, the organic residues could promote to form the porous ceramics for the one-step pyrolyzed powders and XRD patterns show complete perovskite phase of the ceramics sintered at 1,100–1,150 °C for 2 h. The pores are homogeneous dispersion and the ceramics have uniform fine-grain structures with individual grain of 1–3 μm in size.

Acknowledgement This work was supported by the fund of the State Key Laboratory of Solidification Processing in Northwestern Polytechnical University (NPU), China.

References

1. Doran DG (1968) *J Appl Phys* 39:40
2. Halpin WJ (1966) *J Appl Phys* 37:153
3. Guo WP, Datye AK, Ward TL (2005) *J Mater Chem* 15:470
4. Kakihana M, Okubo T, Arima M, Nakamura Y, Yashima M, Yoshimura M (1998) *J Sol–Gel Sci Technol* 12:95
5. Pechini MP (1967) *USP* 3 330 697
6. Lessing PA (1989) *Am Ceram Soc Bull* 68:1002
7. Tai L-W, Lessing PA (1992) *J Mater Res* 7:511
8. Vaqueiro P, Lopez-Quintela MA (1998) *J Mater Chem* 8:161
9. Kakegawa K, Arai K, Sasaki Y, Tomizawa T (1988) *J Am Ceram Soc* 71:C49
10. Zaghete MA, Varela JA, Cilense M, Paiva-Santos CO, Las WC, Longo E (1999) *Ceram Intern* 25:239
11. Tas AC (1999) *J Am Ceram Soc* 82:1582
12. Gajbhiye NS, Venkataramani PS (2002) *Prog Cryst Growth Charact Mater* 44:127
13. Abreu A, Zanetti SM, Oliveira MAS, Thim GP (2005) *J Eur Ceram Soc* 25:743
14. Qiu S, Fan H, Zheng X (2007) *J Sol–Gel Sci Technol* 42:21
15. Blanco López MC, Fourlaris G, Rand B, Riley FL (1999) *J Am Ceram Soc* 82:1777
16. Petrykin V, Kakihana M (2005) *Handbook of sol–gel science and technology. Processing, characterization and applications, vol I, Sol–Gel processing*. Kluwer Academic Publishers, p 85
17. Tsay J-D, Fang T-T, Gubiotti TA, Ying JY (1998) *J Mater Sci* 33:3721
18. Kakihana M, Nagumo T, Okamoto M, Kakihana H (1987) *J Phys Chem* 91:6128
19. Nakamoto K (1986) *Infrared and Raman spectra of inorganic and coordination compounds*, 4th edn. Wiley, New York, p 231
20. Kakihana M, Yoshimura M (1999) *Bull Chem Soc Jpn* 72:1427
21. Leite ER, Varela JA, Longo E, Paskocimas CA (1995) *Ceram Intern* 21:153
22. Qiu S, Fan H, Yang C, Chen J (2007) *J Am Ceram Soc* 90:3293
23. Yang P, Moore RH, Lockwood SJ, Tuttle BA, Voigt JA, Scofield TW (2003) *SAND* 2003–3866
24. Setchell RE (2003) *J Appl Phys* 94:573